The N-Terminal (1−44) and C-Terminal (198−243) Peptides of Apolipoprotein A-I Behave Differently at the Triolein/Water Interface†

Libo Wang, Ning Hua, David Atkinson, and Donald M. Small*

Department of Physiology and Biophysics, Boston University School of Medicine, Boston, Massachusetts 02118

Received May 24, 2007; Revised Manuscript Received August 8, 2007

ABSTRACT: Apolipoprotein A-I (apoA-I), the major protein of high-density lipoprotein (HDL), moves between HDL and triacylglycerol-rich lipoproteins during metabolism. We reported that apoA-I is conformationally flexible at the triolein/water (TO/W) interface, partially desorbing at low surface pressure (Π) but totally desorbing at $\Pi > 19$ mN/m. We now report the different behavior of the N- and C-terminal peptides of apoA-I ([1−44]apoA-I and [198−243]apoA-I) at the TO/W interface. While both peptides are surface active, [198−243]apoA-I is more stable at the TO/W interface. At equilibrium interfacial tension both peptides desorb from the interface when compressed, but [1−44]apoA-I is pushed off at 13 mN/m while [198−243]apoA-I can withstand $\Pi = 16$ mN/m. Neither peptide is very elastic or flexible at the interface. Only at small changes of area (<8%), fast oscillations (4 and 8 s periods), and relatively low concentrations (2×10^{-7} M) do these peptides show elastic behavior but with a relatively small modulus compared to that of apoA-I. When mixed together, they appear not to interact on the surface. [1−44]ApoA-I binds more rapidly but is replaced by [198−243]apoA-I within minutes. We suggest that when apoA-I partially desorbs from lipoprotein surfaces during lipid metabolism, the N-terminal is the first to detach while the C-terminal remains on the interface and only desorbs at higher pressures. Thus, the observations that different domains of apoA-I adsorb or desorb with small variations in surface pressure make apoA-I a very flexible protein with multiple functions, one of which is to stabilize surface pressure during lipoprotein metabolism as lipids move in and out of the lipoprotein surface.

Apolipoprotein A-I (apoA-I)[1] is the major protein of high-density lipoprotein (HDL) and serves to stabilize the HDL particles. Reduced plasma levels of HDL and apoA-I are the key risk factors for atherosclerosis and cardiovascular disease (*1*). The antiatherogenic function of apoA-I is mainly related to its critical role in reverse cholesterol transport during which apoA-I promotes phospholipid and cholesterol efflux from tissues by binding to specific ATP binding cassette (ABC) transporters, activates lecithin:cholesterol acyltransferase (LCAT) to form HDL cholesterol esters (CEs), binds to some lipid transfer proteins to transfer lipids between lipoproteins and thus remodel them, and finally binds to scavenger receptor class B type 1 (SR-B1) to selectively deliver cholesterol and CE to the liver for excretion into bile (*2*−*4*).

ApoA-I moves and exchanges among HDLs and triacylglycerol (TAG)-rich lipoprotein particles such as very-low-density lipoproteins (VLDLs) and chylomicrons (CMs) during lipoprotein metabolism (*5*). It exists in at least three states during metabolism: (a) lipid free or lipid poor in plasma, (b) lipid bound on a discoidal nascent HDL particle that consists of a bilayer of phospholipids and free cholesterol stabilized by apoA-I, and (c) lipid bound at the surface of a spherical lipoprotein particle (HDL or VLDL) that consists of an apolar core of CEs and/or triglycerides (TGs) and a surface of phospholipids and free cholesterol (*6*). The conformational flexibility of apoA-I allows it to adapt to both the polar environment in plasma and the apolar environment on lipoprotein particles and is essential for its multiple functions. It is believed that apoA-I interacts primarily with the phospholipid hydrocarbon chains on discoidal HDL and perhaps spherical HDL, and it is possible that it also interacts with the hydrophobic core of HDL particles and with the hydrophobic TG core of VLDLs and CMs.

ApoA-I has an N-terminal (1−43) domain encoded by exon 3 followed by 10 11/22-mer tandem repeat amino acid segments encoded by exon 4. These repeats are predicted to form type A amphipathic α-helices (*7*, *8*) that are thought to serve as the lipid binding motif of apoA-I and act to stabilize the lipoprotein surface. Sequence analysis (*9*), crystal structures of truncated and full-length apoA-I (*10*, *11*), and NMR assignments (*12*, *13*) all confirm the high α-helical content of apoA-I but differ somewhat on where helical segments are positioned within the primary sequence.

† This work is supported in part by Grant NIH-NHLBI 2P01 HL26335-21.

* To whom correspondence should be addressed. Phone: (617) 638-4001. Fax: (617) 638-4041. E-mail: dmsmall@bu.edu.

[1] Abbreviations: apoA-I, apolipoprotein A-I; HDL, high-density lipoprotein; ABC transporters, ATP binding cassette transporters; LCAT, lecithin:cholesterol acyltransferase; CE, cholesterol ester; SR-B1, scavenger receptor class B type 1; TAG, triacylglycerol; VLDL, very-low-density lipoprotein; CM, chylomicron; TG, triglyceride; A/W, air/water; PC, phosphatidylcholine; O/W, oil/water; CSP, consensus sequence peptide; TO/W, triolein/water; [1−44]apoA-I, N-terminal (1−44) peptide of apoA-I; [198−243]apoA-I, C-terminal (198−243) peptide of apoA-I; DMPC, dimyristoylphosphatidylcholine; apoE-3, apolipoprotein E-3; apoB, apolipoprotein B; EYPC, egg phosphatidylcholine; DD/W, dodecane/water.

10.1021/bi7010114 CCC: $37.00
Published on Web 10/04/2007

The predicted secondary structure of the N-terminal (1−43) domain of apoA-I varies from a G* helix from residue 8 to residue 33 (*8*) to three antiparallel β-strands from residue 14 to residue 57 (*9*). However, a recent crystal structure of apoA-I (*11*) shows that residues 10−39 form a single amphipathic helix (helix A) packed in a four-helix bundle with three exon 4 derived helices (helices B, C, and E) that is very similar to the four-helix bundle formed by the N-terminal of apoE (*14*).

How apoA-I interacts with phospholipids and combinations of phospholipids together with hydrophobic core lipids (TGs, CEs) has been widely studied (*5*, *15*−*21*) using many different approaches. Deletion mutations (*22*−*24*), synthetic peptides encompassing specific regions (*25*−*27*), and "idealized" designed synthesized model peptides of apoA-I (*28*) have been used to determine the affinity of different segments of apoA-I when it binds to phospholipids. Such studies suggest that different parts of the apolipoprotein might bind with different affinities to lipid or lipoprotein surfaces (*29*, *30*). It is generally agreed that the C-terminal region of apoA-I (residues 185−243) has the highest affinity for phospholipid and plays a critical role in initiating the lipid binding (*22*, *29*−*32*). The N-terminal amphipathic region of exon 4 (residues 44−65) also has a high affinity for phospholipids, while the middle region of apoA-I has a significant but lower affinity (*25*). The N-terminal (residues 1−43) is thought to stabilize the lipid-free apoA-I conformation (*33*), while other research also showed that this region also has a moderate phospholipid binding ability (*26*, *34*).

Phospholipid monolayers spread at an air/water (A/W) interface (*25*, *35*−*43*) have been used as a unique model system to study the interaction between apolipoproteins and their peptides with phospholipids. The exclusion pressure (Π_e), i.e., the lowest surface pressure which prevents penetration of the protein or peptide into a phospholipid monolayer, was used to compare the peptide affinities to the phospholipids. ApoA-I has a Π_e of about 30 mN/m (*35*). The Π_e of eight synthesized tandem repeating 22-mer domains of apoA-I at the egg phosphatidylcholine (PC) A/W interface (*25*) showed that, among the 22-mers, the N- and C-terminal peptides (44−65 and 220−241) exhibited the highest Π_e (28 and 30 mN/m), indicating higher affinity to egg PC, while other central peptides exhibited lower Π_e values (<23 mN/m), indicating lower affinity. A number of consensus sequences of amphipathic α-helices modeling different sequences of apolipoproteins (*17*, *18*, *44*) have been investigated using the Π_e technique as well.

Until now, only a few studies have concerned the surface behavior of apolipoproteins or their consensus peptides on oil/water (O/W) interfaces to mimic core lipid interfaces of lipoproteins (*43*, *45*−*48*). In a previous study (*47*), we investigated the interfacial properties of apoA-I and a synthesized consensus sequence peptide (CSP) of exchangeable apolipoproteins at the triolein/water (TO/W) interface. CSP consists of two 22-residue tandem repeat sequences modeling the central domain of apoA-I. It is expected to comprise two antiparallel 20-residue amphipathic α-helices linked by a four-residue proline-containing turn and is an idealized fundamental structural motif of exchangeable apolipoproteins (*9*, *28*). Our results clearly showed (*47*) that both apoA-I and CSP bind strongly to the TO/W interface. They desorbed from the saturated interface when compressed and readsorbed when the surface was expanded. CSP was ejected from the interface at about 16 mN/m (Π_{max}), while some part of apoA-I was pushed off the interface at ∼15 mN/m (Π_{max}), and the entire protein was expelled above ∼19 mN/m (Π_{off}). This suggested that different parts of apoA-I have different affinities for the triolein interface. In addition, our study showed that apoA-I was more flexible at the TO/W interface than CSP and showed more elasticity even at large compression. We suggested that the apoA-I flexibility and surface pressure mediated desorption and readsorption probably provide lipoprotein stability during metabolic remodeling reactions in plasma (*47*).

To understand more about the lipid association and cooperation of different domains of apoA-I, we explored the surface behavior of the N-terminal (1−44) peptide ([1−44]-apoA-I) and the C-terminal (198−243) peptide ([198−243]-apoA-I) at the TO/W interface. We measured and compared the adsorption isotherms, desorption on compression, readsorption on expansion, and the elastic properties of both the peptides. Such information will be helpful to understand the structure of apoA-I on TAG-rich lipoprotein surfaces and the structural changes that occur during remodeling of lipoproteins in plasma.

EXPERIMENTAL PROCEDURES

Materials. The N-terminal peptide [1−44]apoA-I and the C-terminal peptide [198−243]apoA-I of apoA-I were synthesized at Quality Controlled Biochemical Inc. (Hopkinton, MA) and purified to >95%. The purity was further verified by mass spectroscopy. Stock solutions of both peptides (3−5 mg/mL) were prepared in 2 mM pH 7.4 phosphate buffer. At the peptide concentrations used in these experiments (1×10^{-7} to 2×10^{-5} M), [1−44]apoA-I appears to be monomeric while [198−243]apoA-I is monomeric at low concentration ($<1 \times 10^{-6}$M) and partly self-associated with concomitant folding into an α-helix at higher concentrations (*26*, *27*). To measure the interfacial tension of the TO/W interface with peptide, varied amounts of peptide stocks were added to the aqueous phase to obtain different peptide concentrations (from 1×10^{-7} to 2×10^{-5} M). The pH of the aqueous phase was kept at pH 7.4 with phosphate buffer (2 mM). Triolein (>99% pure) was purchased from Nu-Chek Prep, Inc. (Elysian, MN), and its interfacial tension was 32 mN/m. All other reagents were of analytical grade.

Interfacial Tension Measurement. The interfacial tension of the TO/W interface in the presence of different amounts of [1−44]apoA-I, [198−243]apoA-I, or a mixture of [1−44]-apoA-I and [198−243]apoA-I in the aqueous phase was measured with an I. T. Concept (Longessaigne, France) Tracker oil-drop tensiometer (*49*). Triolein drops (16 μL) were formed in gently stirred pH 7.4 phosphate buffer (6.0 mL) containing a given amount of [1−44]apoA-I, [198−243]apoA-I, or a mixture of [1−44]apoA-I and [198−243]-apoA-I. The interfacial tension (γ) was recorded continuously until it approached an equilibrium level. The surface pressure (Π) was obtained from γ of the interface without peptide (γ_{TO}) minus γ of the interface with peptide (γ_{pep}), i.e., $\Pi = \gamma_{TO} - \gamma_{pep}$. All experiments were carried out at 25 ± 0.1 °C in a thermostated system.

Estimation of the Surface Area per Molecule of Peptide. The equilibrium interfacial tension (γ) was obtained for each

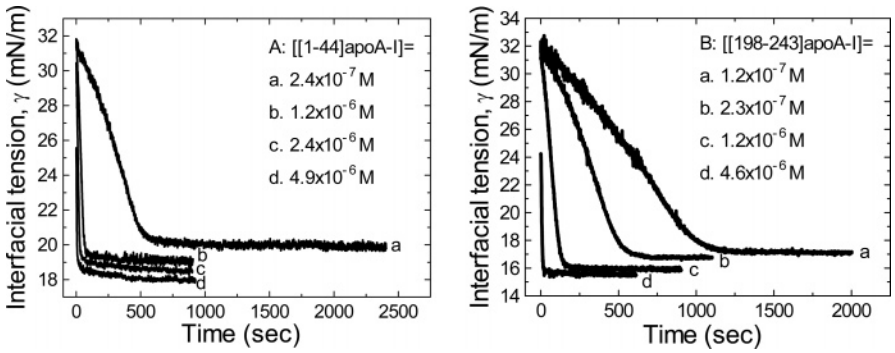

FIGURE 1: Examples of the interfacial tension (γ) plotted against time of [1−44]apoA-I (A) and [198−243]apoA-I (B) at the TO/W interface. A 16 μL triolein drop formed in 2 mM pH 7.4 phosphate buffer with different amounts of peptides. All experiments were carried out at 25 ± 0.1 °C.

concentration (c) of peptide in the aqueous phase. Then γ was plotted against ln c and fitted to a straight line. The slope of the fitted line dγ/(d ln c) gives, according to the Gibbs equation for the surface (*50*), the surface concentration of an adsorbed molecule, Γ (mol/cm^2) = − (1/RT)(dγ/(d ln c))$_{TP}$. The surface area per molecule of peptide (S) was calculated from S (Å^2/molecule) = 1/(ΓN), where N = Avogadro's number.

Instant Compression and Expansion of the Interfaces. Once γ approached an equilibrium level, the oil drop (16 μL) was compressed by rapidly decreasing the volume by as little as 12% (2 μL) or up to 75% (12 μL). The sudden decrease in volume (V) instantaneously decreased the drop surface area (A), resulted in a sudden compression, causing γ to drop abruptly to a certain level, γ_0, and generated an instant surface pressure, $\Pi_0 = \gamma_{TO} - \gamma_0$, where γ_{TO} is the surface tension of pure triolein (32 mN/m). The reduced volume was held for several minutes and γ recorded continuously. Then the surface was expanded by increasing the drop volume back to the original volume and then holding it constant for several minutes. After compression, if peptide molecules readily desorbed from the surface, γ would rise back toward the equilibrium value (the desorption curve). After expansion, if peptide molecules adsorbed from the bulk phase to adhere to the newly formed extra surface, γ would drop back toward the equilibrium γ (the readsorption curve).

Value of Π_{max}. To estimate the maximum pressure (Π_{max}) that peptide could withstand without being ejected from the interface, a series of compression and expansion experiments at different compression and expansion ratios and over a wide range of peptide concentration were carried out. The tension changes ($\Delta\gamma$) over the compression period were plotted against the instant pressure generated right after the compression (Π_0), and the data were fitted to a straight line. The intercept of the straight line at $\Delta\gamma = 0$ gave the Π at which the peptide molecules showed no net adsorption or desorption; this is Π_{max} (*47*, *48*).

Oscillation of the Interface and the Elasticity Analysis. Two types of oscillations were used, oscillations starting at equilibrium γ (γ_e) and continuous oscillations during the adsorption. In equilibrium oscillations the drop volume (16 μL) was sinusoidally oscillated at varied amplitudes (12−75%) and periods (4−128 s) after γ reached an equilibrium level (γ_e). In continuous oscillations the drop volume (16 μL) was sinusoidally oscillated at varied amplitudes (6−25%) and periods (4−32 s) starting several seconds after the drop was formed. While the mean tension (γ) fell toward equilibrium, the area (A) and γ changes were followed as the volume (V) oscillated. In the elasticity analysis, the interfacial elasticity modulus (ϵ = dγ/(d ln A)), the phase angle (ϕ) between compression and expansion, and the elasticity real part (ϵ') and the elasticity imaginary part (ϵ'') were obtained ($\epsilon' = |\epsilon| \cos \phi$, $\epsilon'' = |\epsilon| \sin \phi$) (*51*, *52*). From the $\epsilon-\Pi$ plots, information about the binding and the state of the surface can be gained.

In addition, $\Pi-A$ plots were derived from the oscillations corresponding to the oscillation cycles of the compression and expansion. The $\Pi-A$ plot for a pure elastic surface is a linear curve. The compression and the expansion curves fall on the same line, and ϕ is roughly 0. The $\Pi-A$ plots for a viscoelastic surface usually show a hysteresis between the compression and expansion limbs. The more divergence between the compression and the expansion (i.e., greater phase angle, ϕ) the more viscous the surface.

RESULTS

Adsorption of [1−44]ApoA-I and [198−243]ApoA-I onto the TO/W Interface. Parts A and B of Figure 1 are two typical sets of interfacial tension−time curves of [1−44]apoA-I and [198−243]apoA-I measured at varied peptide concentration in the aqueous phase. Both peptides are surface active and lowered the surface tension (γ) of the TO/W interface (32 mN/m) to reach an equilibrium level. The equilibrium γ was dependent on the peptide concentration in the aqueous phase. The higher the peptide concentration, the lower the equilibrium γ and the less time it took to reach equilibrium. γ of the TO/W interface (32 mN/m) could be lowered by as much as 15 mN/m with 9.7 × 10^{-6} M [1−44]apoA-I in the aqueous phase (curve not shown) and 17 mN/m with 9.3 × 10^{-6} M [198−243]apoA-I in the aqueous phase (curve not shown). The observation that [198−243]apoA-I could lower γ more than [1−44]apoA-I at equivalent concentration indicates that [198−243]apoA-I has a higher affinity for the TO/W interface.

Surface Area per Molecule of [1−44]ApoA-I and [198−243]ApoA-I. The equilibrium γ of [1−44]apoA-I (squares) or [198−243]apoA-I (circles) was plotted against the natural log peptide concentration (ln c), and the data were fitted to a straight line (Figure 2). Usually an area between 14 and 25 Å^2 per residue indicates that the helix is lying flat on the A/W surface (*35*). Our results show that the value for [1−44]-apoA-I is about 15 Å^2 per residue, while that for [198−243]-apoA-I is about 22 Å^2 per residue. Both values are consistent with the peptides lying flat on the TO/W surface.

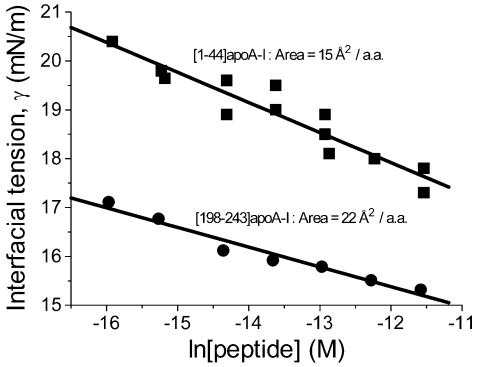

FIGURE 2: Equilibrium interfacial tension (γ) plotted against the natural logarithm of the molar concentration of [1−44]apoA-I (squares) and [198−243]apoA-I (circles) in the aqueous phase. Each point is a separate experiment. Several experiments were carried out at each concentration. The surface area for [1−44]apoA-I was estimated at ∼15 Å²/aa and for [198−243]apoA-I at ∼22 Å²/aa at the TO/W interface.

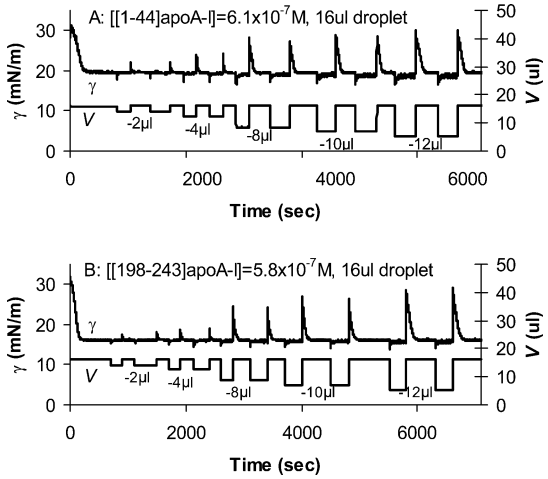

FIGURE 3: Examples of desorption and readsorption curves of [1−44]apoA-I (A) and [198−243]apoA-I (B) at the TO/W interface. A 16 μL triolein drop was compressed at different ratios from 12% to 75% (from 9% to 54% in area) and then after several minutes reexpanded back to the original volume, 16 μL. (A) [1−44]ApoA-I was 6.1×10^{-7} M in the aqueous phase. (B) [198−243]ApoA-I was 5.8×10^{-7} M in the aqueous phase.

Desorption, Readsorption, and the Π_{max} *of [1−44]ApoA-I and [198−243]ApoA-I at the TO/W Interface.* Parts A and B of Figure 3 are example curves for instant compression and expansion of the interface at a given peptide concentration after γ reached an equilibrium level. Figure 3A shows an example for [1−44]apoA-I at a concentration of 6.1×10^{-7} M. After γ approached an equilibrium level, the 16 μL triolein drop was compressed by decreasing the volume by 2, 4, 8, 10, and 12 μL. Every instant compression made γ decrease, but then γ rapidly returned to the equilibrium value. The drop was then expanded to 16 μL, and every expansion made γ increase immediately. Then it returned back to the equilibrium value. Smaller compression induced a smaller change in γ, while larger compression induced a slightly greater fall in γ. At smaller compressions such as a 2 μL compression, γ dropped from 19.7 to 17.8 mN/m, while, at bigger compressions such as a 12 μL compression, the tension dropped to 16.6 mN/m. The observation that after every compression γ decreased first and then returned back to the equilibrium value very quickly indicated that the peptide rapidly desorbed from the surface on rapid compression. On the other hand, expansion after a bigger compression induced a larger increase in γ. When the surface was reexpanded after a large compression, γ rose to a value almost as high as that of an almost empty interface (∼32 mN/m) and then dropped to the equilibrium level again. For example, on expansion from 4 to 16 μL γ immediately rose to 29.6 mN/m and then gradually dropped back to 19.7 mN/m. This indicated that most of the [1−44]apoA-I was pushed off the interface by the 12 μL compression. For example, reducing the drop V from 16 to 4 μL reduced the drop A by 54%. Thus, when γ_e was reached after compression, only about 46% of the molecules were left on the surface, so that when the surface was expanded to 16 μL, the empty space allowed the peptide to readsorb from the aqueous phase. The tension never fell more than ∼3 mN/m even at the largest compression, indicating that the peptide was being expelled from the interface even during the rapid compression.

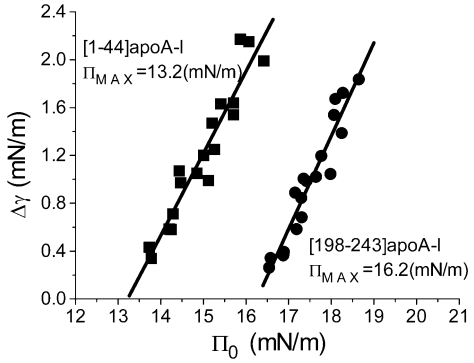

FIGURE 4: Π_{max} of [1−44]apoA-I and [198−243]apoA-I at the TO/W interface. The interface was suddenly compressed to pressure Π_0 and the change in the interfacial tension ($\Delta\gamma$) followed for several minutes. $\Delta\gamma$ was plotted against Π_0, and the data were fitted to a straight line. The intercept of the fit lines at $\Delta\gamma = 0$ gives Π_{max} at which peptides show no net desorption or adsorption. Π_{max} of [1−44]apoA-I at the TO/W interface is 13.2 mN/m, while Π_{max} of [198−243]apoA-I at the TO/W interface is 16.2 mN/m.

[198−243]ApoA-I behaved in a similar way (Figure 3B). The [198−243]apoA-I concentration in Figure 3B was 5.8×10^{-7} M. At smaller compressions (2 μL) little change in the tension was detected, while at bigger compressions (12 μL) the tension dropped from 16.0 to 13.7 mN/m. When expanded from 4 back to 16 μL, γ rose to 29.1 mN/m and then fell back toward the equilibrium γ. This result suggests that, like [1−44]apoA-I, [198−243]apoA-I is also very easily ejected from the interface on compression and rapidly readsorbed when the surface is expanded.

Instant compression followed by reexpansion measurements were made at varied peptide concentrations to get the Π_{max} values for both peptides. Figure 4 shows that Π_{max} of [1−44]apoA-I is 13.2 mN/m and Π_{max} of [198−243]apoA-I is 16.2 mN/m. A higher Π is needed to push off [198−243]apoA-I, indicating that [198−243]apoA-I binds to the triolein/water interface more tightly.

Oscillations and Elasticity Analysis of [1−44]ApoA-I and [198−243]ApoA-I. Both equilibrium and continuous oscillation experiments of [1−44]apoA-I and [198−243]apoA-I at several peptide concentrations and different oscillation conditions (amplitudes and periods) were carried out. Figure 5A shows a set of $\Pi-A$ curves of [198−243]apoA-I which

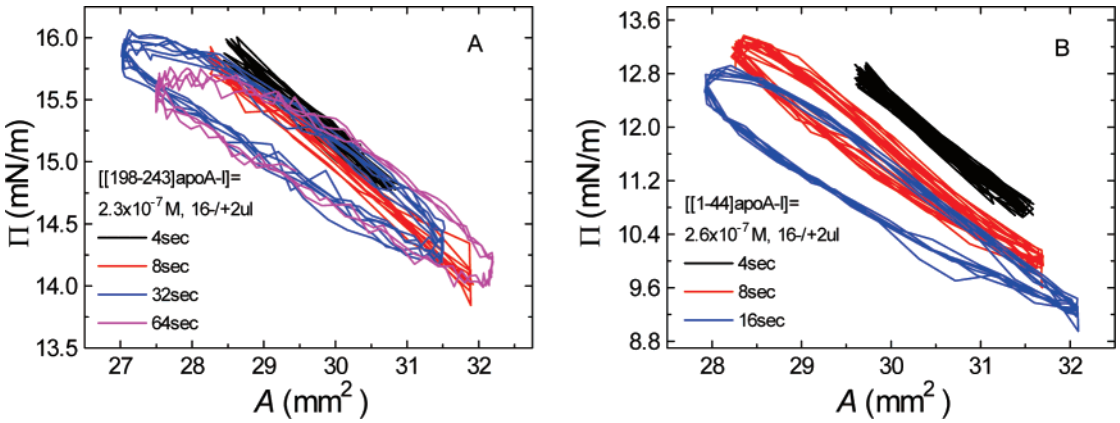

FIGURE 5: Surface pressure (Π) versus area plots of [198−243]apoA-I (A) and [1−44]apoA-I (B) at the TO/W interface. After the equilibrium tension (γ_e) was reached, a 16 μL triolein drop was oscillated at 16 ± 2 μL and different periods from 4 to 64 s. (A) The concentration of [198−243]apoA-I in the aqueous phase was 2.3 × 10^{-7} M. (B) The concentration of [1−44]apoA-I in the aqueous phase was 2.6 × 10^{-7} M.

Table 1: Dynamic Interfacial Properties of [1−44]ApoA-I at the TO/W Interface[a]

$V + \Delta V$ (μL) (design)	$V + \Delta V$ (μL) (actual)	$A + \Delta A$ (mm²)	change in A (%)	period (s)	mean γ (mN/m)	ϵ (mN/m)	ϕ (deg)	ϵ' (mN/m)	ϵ'' (mN/m)
16 ± 2	16.3 ± 0.7	30.5 ± 0.9	±3.0	4	20.2	33.4	−1.3	33.4	−0.8
16 ± 2	15.8 ± 1.4	30.0 ± 1.7	±5.7	8	20.6	29.5	8.4	29.1	4.3
16 ± 2	16.0 ± 1.6	30.0 ± 2.0	±6.7	16	21.1	25.7	14.6	24.9	6.5
16 ± 2	16.2 ± 1.9	29.8 ± 2.4	±8.1	32	19.5	21.4	20.9	20.0	7.6
16 ± 2	16.2 ± 1.9	39.9 ± 2.4	±8.0	128	18.9	13.0	43.5	9.4	8.9
16 ± 4	16.1 ± 1.7	30.1 ± 2.2	±7.3	8	21.0	27.9	6.8	27.6	3.3
16 ± 4	16.0 ± 3.0	29.8 ± 3.8	±12.8	16	21.5	23.1	10.3	22.7	4.1
16 ± 4	16.2 ± 3.4	29.7 ± 4.3	±14.5	32	20.2	21.4	14.1	20.7	5.2
16 ± 4	16.2 ± 3.4	29.7 ± 4.3	±14.5	128	19.5	15.7	34.3	12.9	8.8

[a] All oscillation experiments were carried out on the TO/W interface in 2 mM pH 7.4 phosphate buffer at 25 ± 0.1 °C. [[1−44]apoA-I] = 2.6 × 10^{-7} M. Definitions: V, initial drop volume; ΔV, oscillation amplitude; mean γ, mean interfacial tension of near-equilibrium oscillation; ϵ, viscoelastic modulus; ϕ, viscous phase angle, a phase difference between dγ and dA; ϵ', elastic component, the real part of the modulus; ϵ'', viscous elastic component, the imaginary part of the modulus.

Table 2: Dynamic Interfacial Properties of [198−243]ApoA-I at the TO/W Interface[a]

$V + \Delta V$ (μL) (design)	$V + \Delta V$ (μL) (actual)	$A + \Delta A$ (mm²)	change in A (%)	period (s)	mean γ (mN/m)	ϵ (mN/m)	ϕ (deg)	ϵ' (mN/m)	ϵ'' (mN/m)
16 ± 2	16.2 ± 0.9	29.5 ± 1.1	±3.7	4	16.6	14.6	−5.3	14.5	−1.4
16 ± 2	16.4 ± 1.4	29.8 ± 1.8	±6.0	8	17.0	14.5	1.7	14.5	3.70.4
16 ± 2	15.8 ± 1.8	29.0 ± 2.2	±7.6	32	17.0	11.2	16.0	10.8	4.03.1
16 ± 2	16.3 ± 1.8	29.6 ± 2.6	±8.8	64	17.0	10.2	20.1	9.5	3.5
16 ± 4	15.8 ± 1.8	28.8 ± 2.3	±8.0	8	17.1	13.8	3.6	13.8	0.9
16 ± 4	16.4 ± 3.4	29.3 ± 4.4	±15.0	32	17.7	13.0	12.0	12.7	2.7

[a] All oscillation experiments were carried out on the TO/W interface in 2 mM pH 7.4 phosphate buffer at 25 ± 0.1 °C. [[198−243]apoA-I] = 2.3 × 10^{-7} M. Definitions: V, initial drop volume; ΔV, oscillation amplitude; mean γ, mean interfacial tension of near-equilibrium oscillation; ϵ, viscoelastic modulus; ϕ, viscous phase angle, a phase difference between dγ and dA; ϵ', elastic component, the real part of the modulus; ϵ'', viscous elastic component, the imaginary part of the modulus.

were derived from the oscillations at 16 ± 2 μL and periods from 4 to 64 s. Only at short periods of 4 and 8 s were Π−A curves linear, suggestive of an elastic surface, while at longer periods, hysteresis between the compression and the expansion limbs was present, which indicated a viscoelastic surface. Figure 5B shows similar trends in a set of Π−A curves of [1−44]apoA-I that were derived from the oscillations at 16 ± 2 μL and periods from 4 to 16 s. Plots derived from larger amplitude (16 ± 4, 8, and 12 μL) oscillations for both peptides showed a much bigger hysteresis, indicating a more viscous component was added to the system (data not shown).

Oscillations at different amplitudes, different periods, and varied peptide concentrations were carried out thoroughly. The elasticity analysis data for [1−44]apoA-I at 2.6 × 10^{-7} M are listed in Table 1, while the data for [198−243]apoA-I at 2.3 × 10^{-7} M are listed in Table 2. In comparison with other peptides (the consensus sequence peptide of apoB, P12, P27, and the consensus peptide of apoA-I, CSP) and proteins (apoA-I and apoB) that we have studied (*45*−*48*), both [198−243]apoA-I and [1−44]apoA-I have a relatively low modulus (<15 and <35 mN/m, respectively) with a relatively large phase angle (over 40° in some cases), which indicates that both [198−243]apoA-I and [1−44]apoA-I behaved in a rather viscoelastic manner. Only at very short periods (4 or 8 s) and a very small area change (<8%) did the peptides show elastic behavior (phase angles <10°). However, both [1−44]apoA-I and [198−243]apoA-I still roughly follow the rules we established in our previous studies (*45*, *47*) that the bigger the amplitude, the longer the period, the smaller

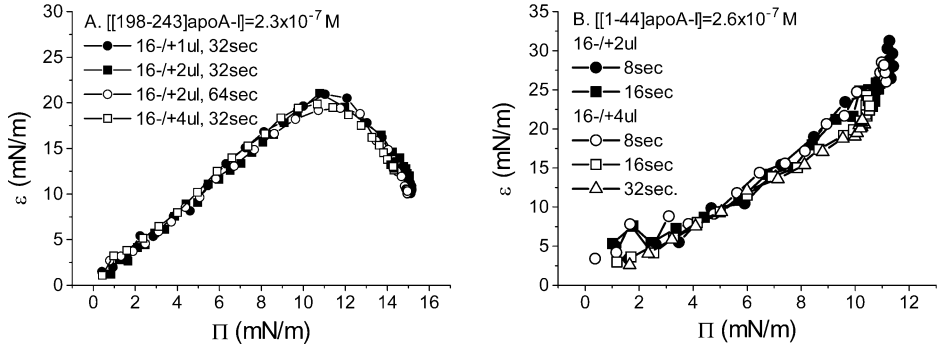

FIGURE 6: Elasticity modulus (ϵ) versus surface pressure (Π) plots for [198−243]apoA-I (A) and [1−44]apoA-I (B) at TO/W interface. Data derived from continuous oscillations at varied amplitudes and periods are very similar for the same peptide but are different between [1−44]apoA-I and [198−243]apoA-I. (A) [198−243]apoA-I was 2.3×10^{-7}M in aqueous phase; (B) [1−44]apoA-I was 2.6×10^{-7}M in aqueous phase.

the modulus, and the bigger the phase angle, indicating a relatively more viscous system.

The simplest explanation for the nonelastic part of the modulus or imaginary elastic modulus (ϵ'') is that the peptide is pushed off the surface on compression and readsorbs in expansion so $A\Gamma$ is not constant as it should be in an elastic surface.

The modulus versus surface pressure ($\epsilon-\Pi$) plots were derived from continuous oscillations for [198−243]apoA-I (Figure 6A) and [1−44]apoA-I (Figure 6B), corresponding to oscillations at varied amplitudes and varied periods. For each peptide, despite different amplitudes and periods, the $\epsilon-\Pi$ plots were similar. However, the plots were different between the two peptides, which indicates that the two peptides behave differently at the TO/W interface. There are two regions on the [198−243]apoA-I plots (Figure 6A). When the surface pressure is between 0 and 11 mN/m, the plot is linear and shows a 2:1 modulus (ϵ) to pressure (Π) ratio, a ratio characteristic of an elastic surface (*51*, *52*). However, when the pressure is greater than 12 mN/m, ϵ decreases sharply, indicating a major change at the interface. We speculate that since the C-terminal peptide self-associates at high concentrations in the bulk aqueous phase that compression at pressures beyond about 10 mN/m may cause some surface self-association and give rise to a collapselike phenomenon of aggregates between 10 and 15 mN/m before being ejected from the surface. This change is not seen on the [1−44]apoA-I plots (Figure 6B). [1−44]ApoA-I simply shows a linear change with the ideal 2:1 ratio for an elastic surface till the pressure reaches 10 mN/m. At 12 mN/m, the molecules were pushed off the surface with the high Π end of each oscillation and were lost from the surface.

Adsorption of Mixtures of [1−44]ApoA-I and [198−243]-ApoA-I onto the TO/W Interface. To investigate how [1−44]-apoA-I and [198−243]apoA-I interact with each other on the TO/W interface, we added equal amounts of [1−44]-apoA-I and [198−243]apoA-I (1.2×10^{-6} M each) to the aqueous phase and compared the γ−time curves with those of the individual peptides. Figure 7 shows the tension−time curves of [1−44]apoA-I (1.2×10^{-6} M), [198−243]apoA-I (1.2×10^{-6} M), and the mixture of [1−44]apoA-I and [198−243]apoA-I. By 90 s, γ fell to 19.0 mN/m with [1−44]apoA-I (curve a), while [198−243]apoA-I lowered γ to 15.9 mN/m by 160 s (curve b). The mixture of [1−44]apoA-I and [198−243]apoA-I lowered the tension to 15.7 mN/m (curve c). In the first part of curve c, the tension fell rapidly to

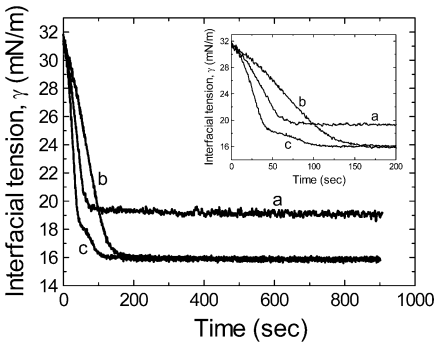

FIGURE 7: Interfacial tension versus time curves for [1−44]apoA-I, [198−243]apoA-I, and the mixture of [1−44]apoA-I and [198−243]apoA-I. (a) [1−44]ApoA-I was 1.2×10^{-6} M in the aqeous phase. (b) [198−243]ApoA-I was 1.2×10^{-6} M in the aqeous phase. (c) Equal amounts of [1−44]apoA-I (1.2×10^{-6} M) and [198−243]apoA-I (1.2×10^{-6} M) were mixed together in the aqueous phase. The inset shows the tension versus time curves in the 0−200 s region.

∼18.5 mN/m. The shape and the slope of the curve in this part are very similar to those of the first part of curve a. Then the tension fell slowly with a shape and slope similar to those of the same part in curve b. Finally, curve c reached equilibrium at the same level as curve b. This result suggests that when the mixture of [1−44]apoA-I and [198−243]apoA-I was added to the aqueous phase, [1−44]apoA-I adsorbed more rapidly onto the interface and lowered γ toward ∼19 mN/m, and then [1−44]apoA-I was displaced by [198−243]apoA-I, causing γ to fall gradually to the equilibrium tension of [198−243]apoA-I. This is consistent with [198−243]apoA-I having a higher affinity for the TO/W interface, displacing [1−44]apoA-I with time. In other words, [1−44]-apoA-I adsorbs onto the interface faster, while [198−243]-apoA-I makes the interface more stable.

Instant compression and expansion experiments with the mixture of [1−44]apoA-I and [198−243]apoA-I in the aqueous phase were carried out, and the Π_{max} value was measured. The data points of the $\Delta\gamma-\Pi_0$ curve for the mixture were very similar to those for [198−243]apoA-I (see Figure 4) and different from those for [1−44]apoA-I (data not shown). Elasticity analysis by equilibrium oscillations for the mixture was also similar to that of [198−243]apoA-I but not that of [1−44]apoA-I. These results suggest that the interface was occupied with [198−243]apoA-I when it reached an equilibrium level.

DISCUSSION

The lipid binding functions of apoA-I and individual segments of apoA-I suggest that different parts of this apolipoprotein might bind with different affinities to lipid or lipoprotein surfaces (*29*−*33*, *47*).

First, lipid monolayers spread at an A/W interface have been used to study the affinity of apolipoproteins and their fragment peptides for various phospholipid or phospholipid/cholesterol monolayers (*25*, *35*−*43*). This technique models binding of peptides to a flat putative lipoprotein surface and gives an important assessment of peptide penetration into and binding to the monolayer. The N-terminal 1−33 aa region with a Π_e of 27 mN/m shows a moderate lipid binding affinity to the egg PC monolayer, while the C-terminal [220−241]apoA-I binding is greater (30 mN/m). While the N- and C-terminal are shorter than those studied in this work, the trend is similar; i.e., the C-terminal binds more strongly than the N-terminal (*25*, *34*).

A second technique mixes peptide with multilamellar surface lipid vesicles, follows the rate of clearing, and observes the size and shape and the inferred structure of the stabilized particles (*5*, *15*−*21*). These studies give information about the kinetics of interaction and the type of particle formed. Zhu and Atkinson (*26*, *27*) demonstrated that [1−44]-apoA-I interacts with dimyristoylphosphatidylcholine (DMPC) over a wide range of lipid:peptide ratios to form ∼100 Å diameter disklike particles that coexist with a heterogeneous population of lipid vesicles at high ratios. Compared to the unfolded structure in solution, [1−44]apoA-I has 60% α-helical content on both the disklike particles and vesicles. In contrast, the C-terminal [198−243]apoA-I showed a very strong affinity for DMPC and formed two sizes of discoidal HDL-like particles (110 and 165 Å) depending on the initial lipid:peptide ratio. Both complexes are similar to those of plasma apoA-I/DMPC complexes, which suggests that the C-terminal peptide may be responsible for apoA-I function in the formation and maintenance of HDL subspecies in plasma.

A third strategy uses preformed lipid emulsions of defined composition and size as model lipoproteins to study peptide binding (*5*, *29*, *30*). This has the advantage that the model emulsions contain core molecules (e.g., TAG or CE) as well as surface molecules. The idea that certain domains of an apolipoprotein might desorb leaving another domain attached (*53*) was tested on egg phosphatidylcholine (EYPC)/TO emulsions for apoE-4 (*54*). Saito et al. showed that both N- and C-terminals of apoE-4 were bound to EYPC/TO emulsions at low protein saturation but that the N-terminal detached at high protein concentration, leaving the peptide attached by the C-terminal. We suggested that the N-terminal desorption might be mediated by an increased surface pressure produced by an increase in peptide concentration at the EYPC/TO interface (*47*), but the changing surface pressure is difficult to estimate in emulsion systems (*47*, *55*). A similar concept of N-terminal dissociation has been put forward for apoA-I (*29*, *30*).

It is reasonably assumed that apoA-I and other apolipoproteins interact with the surface-located phospholipids, but it is also possible that they interact with core molecules such as TAG or CE. Certainly, when the number of surface lipid molecules is too small to adequately cover the core, then apolipoproteins must fill in to stabilize the surface.

Until recently, most of the quantitative research on apolipoproteins on interfaces has been carried out at the A/W interface. Only a few studies have looked at surface behavior of apolipoproteins or their consensus peptides on the O/W interfaces to mimic core lipid interfaces of lipoproteins (*43*, *45*−*48*). Using a novel surface technique of oil drop tensiometry, we have studied the interfacial properties of apoA-I and a synthesized 44-residue CSP modeling the exon 4 domain of apoA-I at the TO/W interface (*47*) and at dodecane/water (DD/W) and A/W interfaces (*45*). We measured the adsorption isotherms, studied the desorption and readsorption behaviors, and analyzed the elasticity properties of apoA-I and CSP to describe how they interact with hydrophobic interfaces (TO/W, A/W, and DD/W). Our results (*47*) showed that CSP binds strongly to these surfaces but is pushed off at high pressure (Π_{max} = 16 mN/m for TO/W). ApoA-I also binds to the TO/W interface. A part of apoA-I is expelled from the surface at ∼15 mN/m but can snap back on rapidly. The whole apoA-I molecule desorbed into the aqueous solution when compressed above 19 mN/m. Furthermore, apoA-I showed greater elasticity on the surface than CSP, indicating a great flexibility. Therefore, apoA-I has different parts which bind more or less tightly to the surface, which allows it a great flexibility over a fairly narrow surface pressure range (15−20 mN/m). We suggested that the apoA-I flexibility and surface pressure mediated desorption and readsorption probably provide lipoprotein stability during metabolic remodeling reactions in plasma.

To continue to explore the interaction between different domains of apoA-I and a lipoprotein corelike interface (TO/W), we studied the surface behavior of the exon 3 coded N-terminal peptide [1−44]apoA-I and the C-terminal peptide [198−243]apoA-I and compared them to CSP and the whole apoA-I.

Our studies show that both N- and C-terminal peptides are surface active and lower the interfacial tension of the TO/W interface in a time- and concentration-dependent fashion (Figure 1). At each given concentration an equilibrium γ is reached that decreases with the natural log of the concentration in a linear fashion that allows the interfacial concentration and area for the peptides to be estimated from the Gibbs absorption isotherm (see the Experimental Procedures). Both peptides have reasonable surface areas of ∼15 and ∼22 Å^2 per amino acid for [1−44]apoA-I and [198−243]apoA-I, respectively (Figure 2). These areas are in the same range as those measured by several other studies (*45*) and are consistent with the area of α-helices lying flat on an interface. [198−243]ApoA-I, however, is more surface active and has a higher affinity to the TO/W interface than [1−44]-apoA-I. It lowers the interfacial tension at its maximum concentration (∼9.7 × 10^{-6} M) to about 15 mN/m, while [1−44]apoA-I does not fall below 17 mN/m at an equivalent concentration (∼9.3 × 10^{-6} M).

Both [1−44]apoA-I and [198−243]apoA-I desorbed rapidly from the interface upon instant compression as shown by the rapid return to the equilibrium γ. Upon instant expansion they readsorbed to the interface rapidly to reestablish the equilibrium γ (Figure 3). Following a large compression (12 μL, ∼54% in area), reexpansions caused γ to rise to ∼30 mN/m, indicating a very low surface

concentration. This means that a large fraction of the peptide was pushed off the surface at the compression stage. Upon compression of both peptides, the tension did not drop much from equilibrium and returned back to equilibrium very quickly, indicating a very fast desorption process to maintain an equilibrium surface with the same surface concentration. In our previous study (*47*), CSP and apoA-I showed very different desorption curves, in which the tension dropped first and then rose more slowly back to a certain level but not to the equilibrium level within 10 min after compression. This suggests that CSP and apoA-I could stay compressed on the surface with a higher surface concentration, while [1−44]apoA-I and [198−243]apoA-I cannot stand a compression state beyond their equilibrium γ and are more easily pushed off the surface.

[1−44]ApoA-I and [198−243]apoA-I differ in the desorption process in terms of the Π_{max} value, the pressure at which the peptide begins to be forced off the surface into the aqueous phase. Π_{max} of [198−243]apoA-I is about 3 mN/m higher than that of [1−44]apoA-I (16.2 vs 13.2 mN/m). Thus, [1−44]apoA-I is a good candidate for early detachment from the lipoprotein as the pressure moves above 13 mN/m, whereas [198−243]apoA-I appears to remain bound at relatively higher pressures.

The adsorption isotherm of the mixture of an equal amount of [1−44]apoA-I and [198−243]apoA-I showed a combined behavior of the two (Figure 7). It appears that the [1−44]-apoA-I bound more quickly to the TO/W interface and then was replaced by [198−243]apoA-I within 2 min. There is no evidence that [198−243]apoA-I and [1−44]apoA-I interacted with each other. Data on desorption and readsorption, the Π_{max} value, and elasticity analysis (data not shown) of the mixture of the two peptides are all consistent with the suggestions that [198−243]apoA-I is more stable on the interface than [1−44]apoA-I.

[1−44]ApoA-I and [198−243]apoA-I also present somewhat different $\epsilon-\Pi$ plots derived from continuous oscillation experiments. The maximum ϵ occurs for both at a Π of ~12 mN/m, but ϵ is significantly greater for [1−44]apoA-I than [198−243]apoA-I (~33 vs 20 mN/m). Since [1−44]-apoA-I has a higher surface density (1 aa/15 Å) than [198−243]apoA-I (1 aa/22 Å), an equal increase in Π should give rise to a larger ϵ for the N-terminal. At pressure up to ~10 mN/m both peptides behave elastically and have a $d\epsilon/d\Pi \approx 2$. Above 10 mN/m the ϵ of [1−44]apoA-I rose abruptly to ~33 mN/m, while that of [198−243]apoA-I plateaus at ~20 mN/m and then falls at higher pressures, suggesting some nonelastic change in the surface. We noted that, in solution, at a concentration of $(2.3-2.6) \times 10^{-7}$ M both peptides are monomeric, but [198−243]apoA-I tends to self-associate at concentrations above 1×10^{-6} M, while [1−44]apoA-I is monomeric up to almost 1×10^{-4} M (*26*, *27*). It is possible that when [1−44]apoA-I and [198−243]-apoA-I bind to the TO/W interface, [1−44]apoA-I remains monomeric while [198−243]apoA-I molecules interact with each other to form surface aggregates when the surface concentration is increased as Π becomes greater than ~10 mN/m. This putative surface−peptide interaction might explain the collapselike region between $\Pi = 12$ mN/m and $\Pi = 16$ mN/m seen in the $\epsilon-\Pi$ plot (Figure 6A) of [198−243]apoA-I.

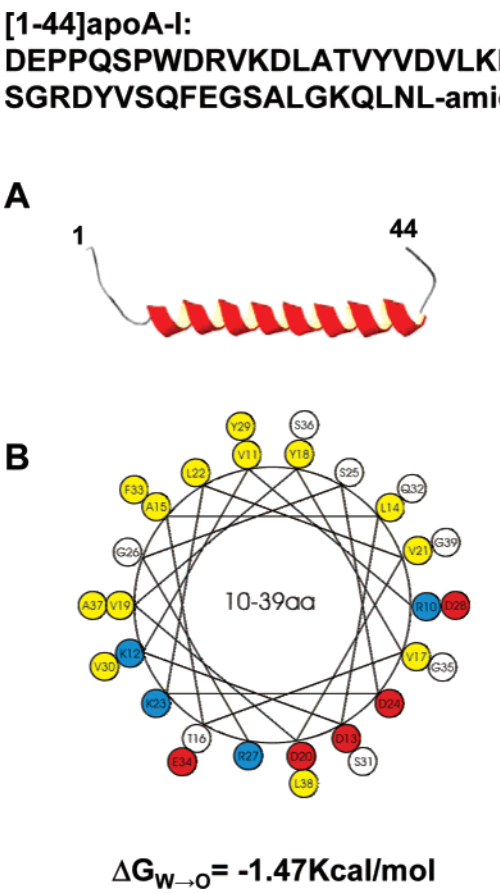

FIGURE 8: Amino acid sequence, structure (A), and α-helical wheel (B) of residues 1−44 of apoA-I. The structure of residues 1−44 was adapted from the crystal structure of full-length apoA-I (*11*) and presented in Swiss-PDBViewer. According to the crystal structure determination (*11*), [1−44]apoA-I contains an α-helical structure from 10 to 39, so the α-helical wheel was drawn for residues 10−39. The hydrophobic residues are in yellow, the basic residues are in blue, the acidic residues are in red, and all other residues are without color. The mean ΔG for moving the hydrophobic face from the water phase to the oil phase ($\Delta G_{W\rightarrow O}$) was calculated on the basis of this helical structure from residues 10 to 39 and is −1.47 kcal/mol.

At surface saturation, [1−44]apoA-I and [198−243]apoA-I are both rather inelastic and easy to displace from the surface, while apoA-I is more elastic and flexible (*47*). Both [1−44]apoA-I and [198−243]apoA-I tend to have larger phase angles and smaller modulus at similar changes in area compared to apoA-I.

Part of the different behaviors of [1−44]apoA-I and [198−243]apoA-I at the interface can be explained by the differences in the change in surface free energy which occurs when the peptides bind to the TO/W interface. At the peptide concentrations used in these experiments (1×10^{-7} to 2×10^{-5} M), [1−44]apoA-I appears to be monomeric, while [198−243]apoA-I is monomeric at low concentration ($<1 \times 10^{-6}$ M) and partly self-associates with concomitant folding into an α-helix at higher concentrations (*26*, *27*). The surface tension (γ) of the TO/W interface (~32 mN/m) is reduced when the peptide binds, and the change in free energy can be roughly estimated from $\Delta\Delta G_{TO} = (\Delta\gamma)(\Delta A)$, where $\Delta\gamma$ is the change in γ from that of a pure TO surface (32 mN/m) to the γ with peptide bound to the TO surface. The increment in area (ΔA) can be estimated by the surface area occupied by the amphipathic α-helix at the interface,

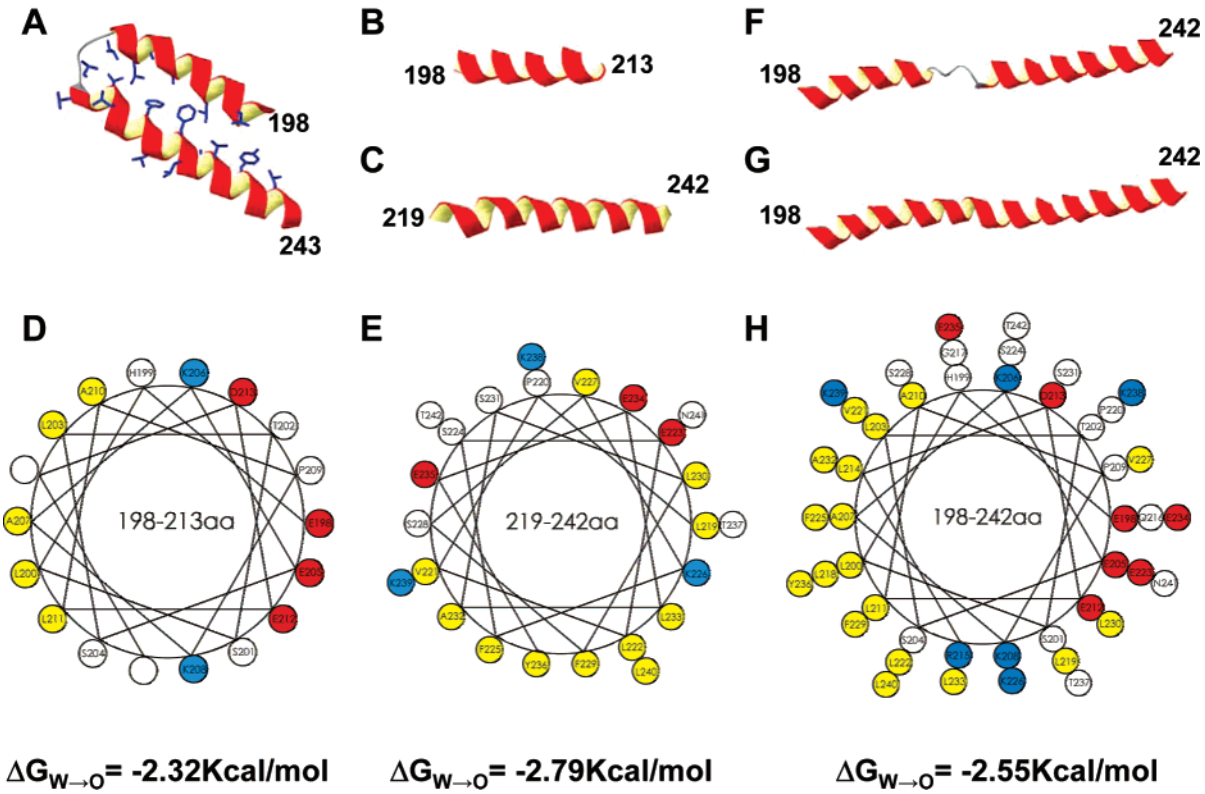

FIGURE 9: Amino acid sequence, secondary structures, and α-helical wheels of whole and partial segments in the C-terminal residues 198−243 of apoA-I. The structures of each helix in (A)−(C) were adapted from the crystal structure of full-length apoA-I (*11*) and presented in Swiss-PDBViewer. Secondary structures in (F) and (G) were modeled by using Swiss-PDBViewer. Helical wheels were drawn on the basis of different α-helical segments in the crystal (*11*), and ΔG for moving the hydrophobic face from the water phase to the oil phase ($\Delta G_{W\rightarrow O}$) was calculated accordingly. In helical wheel plots, the hydrophobic residues are in yellow, the basic residues are in blue, the acidic residues are in red, and all other residues are without color. (A) Structure of the C-terminal of apoA-I from residue 198 to residue 243 in the crystal (*11*). The hydrophobic residues are shown as sticks and reside between the two helix bundles. (B) Structure of the first α-helix from residue 198 to residue 213. (C) Structure of the second α-helix from residue 219 to residue 242. (D) Helical wheel for the helical structure from residue 198 to residue 213. $\Delta G_{W\rightarrow O}$ for this helix is −2.32 kcal/mol. (E) Helical wheel for the helical structure from residue 219 to residue 242. $\Delta G_{W\rightarrow O}$ for this helix is −2.79 kcal/mol. (F) Structure modeled as the two-helix bundle between residue 198 and residue 242 opened up as if bound to lipids. (G) Structure modeled assuming that residues from 198 to 242 form a long α-helical structure. (H) Helical wheel assuming helical structure from residue 198 to residue 242 as modeled in (G). This shows a long, type A amphipathic α-helix with a $\Delta G_{W\rightarrow O}$ of −2.55 kcal/mol.

which varies between 15 and 22 Å^2/residue depending on the experiments. When the α-helical peptide is bound to the interface, the amino acids on its hydrophobic face bind to the hydrophobic TO surface. If we assume that roughly half of the amino acids are on the hydrophobic surface, each hydrophobic residue would occupy roughly 30 Å^2 at the TO interface. Thus, for every hydrophobic residue binding to the TO surface, we would lose ∼30 Å^2 of the TO/W interface (i.e., $\Delta A \approx 30$ Å^2). Note that 30 Å^2 also corresponds to the approximate area of one oleate chain in TO at the A/W interface. As a first approximation for [1−44]apoA-I, the minimum surface tension is 17 mN/m, which gives a $\Delta\gamma$ of −15 mN/m. Therefore, the change in free energy in the TO surface on binding of the peptide ($\Delta\Delta G$) would be −0.65 kcal per hydrophobic amino acid residue (30 Å^2). For [198−243]apoA-I, $\Delta\gamma$ is −17 mN/m, which gives a $\Delta\Delta G$ of −0.74 kcal/30 Å. Thus, $\Delta\Delta G$ is slightly more favorable for [198−243]apoA-I than [1−44]apoA-I. To estimate the total energy change on binding, the fact that the hydrophobic amino acids on the putative hydrophobic face are exposed to water in the bulk aqueous system at concentration $<10^{-6}$ M must be considered. If these amino acids are transferred to an oily interface (e.g., TO) and form an amphipathic α-helix, the total free energy of peptide interfacial binding will be reduced further by removing these hydrophobic residues from water. As a rough approximation one can sum the individual free energies for transfer of hydrophobic residues from water to oil ($\Delta G_{W\rightarrow O}$) for all of the amino acids in the putative hydrophobic face of the helix and divide by the number of residues (*56*). According to the crystal structure of the full-length apoA-I (*11*), residues 10−39 form an α-helix structure (Figure 8), giving about 65% helix for [1−44]apoA-I. Thus, for [1−44]apoA-I such a calculation yields $\Delta G_{W\rightarrow O} = -1.47$ kcal/mol of hydrophobic

face residues. Assuming that [198−243]apoA-I is a single, long amphipathic helix (Figure 9G,H), the $\Delta G_{W\rightarrow O}$ of [198−243]apoA-I is −2.55 kcal/mol of hydrophobic face residues or somewhat more favorable than that for [1−44]apoA-I. The total free energy involves the energy gained on removing the 30 Å^2 of pure triglyceride surface from water and covering it with peptide plus the favorable energy obtained by removing the hydrophobic residues from the aqueous phase and placing them in the oily triglyceride surface. Therefore, the total energy gained from [1−44]apoA-I would be approximately −2.1 kcal/mol of hydrophobic amino acids, and that for [198−243]apoA-I would be about −3.3 kcal/mol. Thus, there is a significant difference in calculated favorable energies produced when these peptides bind to the surface. [198−243]ApoA-I binding is clearly energetically more favorable. The differences in the energies probably partly account for the greater pressure (Π_{max}) needed to push [198−243]apoA-I off the interface. It also explains how [198−243]apoA-I can displace the N-terminal peptide at the TO/W interface.

We have shown (*47*) that apoA-I compressed at the TO/W interface starts to be partially displaced at a pressure slightly under 15 mN/m, but cannot be totally ejected from the triolein interface until the pressure is greater than 19 mN/m. We would suggest that one of the first amphipathic regions to be ejected during pressure changes in lipoprotein interfaces involving apoA-I adsorption to core lipids would be the N-terminal, while the C-terminal may serve to partly anchor remaining protein to the interface until higher pressures are reached. The crystal structure of apoA-I by Agees et al. (*11*) shows that the N-terminal [1−44]apoA-I is mainly in an amphipathic α-helical conformation forming helix A (residues 10−39) of the N-terminal four-helix bundle **(**Figure 8**)**. The hydrophobic faces of the four helices (A−D) are packed in the center of the bundle and would have to disaggregate to bind lipid. ApoA-I was crystallized with Cr(acac)$_3$ (*11*). This molecule, chromium(III) tris(acetylacetonate), presents a hydrophobic surface. Cr(acac)$_3$ links leucines 218, 219, and 222, which lie between C-terminal helices E and F, to two other apoA-I molecules to form an apoA-I trimer as part of the unit cell (*11*). The conformation of the C-terminal in the crystal shows tight interaction between hydrophobic faces (Figure 9A) made up of two amphipathic helices (E, F) that pack on one another. Would this conformation exist in the absence of Cr(acac)$_3$? To bind lipid, helices E and F must open up to expose their hydrophobic side to lipid. While the two helices might act separately (Figure 9B,C,F), it is possible that the C-terminal 196−243 in solution might form a single helix incorporating L218, L219, and L222 as part of one long helix (Figure 9G). Helical wheel plots (Figure 9D,E) of the E and F helices show them to be relatively good amphipathic helices with a moderate tendency toward the A type. However, the leucines in the F helix (L219, L230) appear to fall into the polar region and thus would be exposed to solvent. A plot of the entire C-terminal from 196 to 243 as a continuous helix (Figure 9H) shows a relatively striking amphipathic helical wheel with one very hydrophobic face subtending about 120°. Two prolines appear on the hydrophilic face, both of which were present in the crystalline E and F helices (Figure 9D,E). We speculate that a long single helix is formed which is the motif that binds at the TO/W interface.

In summary, both [1−44]apoA-I and [198−243]apoA-I are surface active at the TO/W interface. [198−243]ApoA-I is more stable at the TO/W interface. Both peptides desorb from the interface when compressed, but [1−44]apoA-I is more easily pushed off the interface with Π_{max} of 13 mN/m, while [198−243]apoA-I can stand a higher pressure of 16 mN/m. Neither peptide is very elastic or flexible at the interface. Only at small changes of area (<8%), very fast oscillations (4 and 8 s periods), and relatively low concentrations (2×10^{-7} M) do these peptides show a small phase angle indicating a limited elastic behavior but with a relatively small modulus ϵ compared to those of apoA-I and CSP (*47*). When mixed together, they do not appear to interact with each other on the surface. [1−44]ApoA-I binds more rapidly but is apparently replaced by [198−243]apoA-I within 2 min. They show different adsorption processes. We suggest that when apoA-I detaches from lipoprotein surfaces during lipid metabolism, the N-terminal might be the first part to detach, while the C-terminal will stay on the interface and only detaches at higher pressure at a later stage. Thus, different domains of apoA-I adsorb and desorb upon varied pressure and cooperate with each other to make apoA-I a very flexible protein with multiple functions, one of which is to stabilize surface pressure within a limited range as lipids move in and out of the lipoprotein surface.

ACKNOWLEDGMENT

We thank Donna Ross for manuscript preparation.

REFERENCES

1. Castelli, W. P., Doyle, J. T., Hames, C. G., Hjortland, M. C., Hulley, C. B., Kagan, A., and Zukel, W. J. (1977) HDL cholesterol and other lipids in coronary heart disease. The cooperative lipoprotein phenotyping study, *Circulation 55*, 767−772.
2. Fielding, C. J., and Fielding, P. E. (1995) Molecular physiology of reverse cholesterol transport, *J. Lipid Res. 36*, 211−228.
3. Rye, K. A., and Barter, P. J. (2004) Formation and metabolism of prebeta-migrating, lipid-poor apolipoprotein A-I, *Arterioscler., Thromb., Vasc. Biol. 24*, 421−428.
4. Tall, A. R. (1998) An overview of reverse cholesterol transport, *Eur. Heart J. 19* (Suppl. A), A31−A35.
5. Atkinson, D., and Small, D. M. (1986) Recombinant lipoproteins: implications for structure and assembly of native lipoproteins, *Annu. Rev. Biophys. Biophys. Chem. 15*, 403−456.
6. Small, D. M. (1992) Structure and Metabolism of the Plasma Lipoproteins, in *Current Issues in Endocrinology and Metabolism: Plasma Lipoproteins and Coronary Artery Disease* (Kreisberg, R. A., and Segrest, J. P., Eds.) pp 57−91, Blackwell Scientific Publications, Boston, MA.
7. Segrest, J. P., Jackson, R. L., Morrisett, J. D., and Gotto, A. M., Jr. (1974) A molecular theory of lipid-protein interactions in the plasma lipoproteins, *FEBS Lett. 38*, 247−258.
8. Segrest, J. P., Jones, M. K., DeLoof, H., Brouilette, C. G., Venkatachalapathi, Y. V., and Anantharamaiah, G. M. (1992) The amphipathic helix in the exchangeable apolipoproteins: a review of secondary structure and function, *J. Lipid Res. 33*, 141−166.
9. Nolte, R. T., and Atkinson, D. (1992) Conformational analysis of apolipoprotein A-I and E-3 based on primary sequence and circular dichroism, *Biophys. J. 63*, 1221−1239.
10. Borhani, D. W., Rogers, D. P., Engler, J. A., and Brouillette, C. G. (1997) Crystal structure of truncated human apolipoprotein A-I suggests a lipid-bound conformation, *Proc. Natl. Acad. Sci. U.S.A. 94*, 12291−12296.
11. Ajees, A. A., Anantharamaiah, G. M., Mishra, V. K., Hussain, M. M., and Murthy, H. M. K. (2006) Crystal structure of human apolipoprotein A-I: Insights into its protective effect against cardiovascular diseases, *Proc. Natl. Acad. Sci. U.S.A. 103*, 2126−2131.

12. Okon, M., Frank, P. G., Marcel, Y. L., and Cushley, R. J. (2001) Secondary structure of human apolipoprotein A-I(1−186) in lipid-mimetic solution, *FEBS Lett. 487*, 390−396.
13. Okon, M., Frank, P. G., Marcel, Y. L., and Cushley, R. J. (2002) Heteronuclear NMR studies of human serum apolipoprotein A-I. Part I. Secondary structure in lipid-mimetic solution, *FEBS Lett. 517*, 139−143.
14. Wilson, C., Wardell, M. R., Weisgraber, K. H., Mahley, R. W., and Agard, D. A. (1991) Three-dimensional structure of the LDL receptor-binding domain of human apolipoprotein E, *Science 252*, 1817−1822.
15. Tall, A. R., Small, D. M., Deckelbaum, R. J., and Shipley, G. G. (1977) Structure and thermodynamic properties of high density lipoprotein recombinants, *J. Biol. Chem. 252*, 4701−4711.
16. Pownall, H. J., Massey, J. B., Kusserow, S. K., and Gotto, A. M. Jr. (1979) Kinetics of lipid−protein interactions: effect of cholesterol on the association of human plasma high-density apolipoprotein A-I with L-alpha-dimyristoylphosphatidylcholine, *Biochemistry 181*, 574−579.
17. Brouillette, C. G, and Anantharamaiah, G. M. (1995) Structural models of human apolipoprotein A-I, *Biochim. Biophys. Acta 1256*, 103−129.
18. Brouillette, C. G., Anantharamaiah, G. M., Engler, J. A., and Borhani, D. W. (2001) Structural models of human apolipoprotein A-I: a critical analysis and review, *Biochim. Biophys. Acta 1531*, 4−46.
19. Scanu, A. M. (1972) Structural studies on serum lipoproteins, *Biochim. Biophys. Acta 265*, 471−508.
20. Ritter, M. C., and Scanu, A. M. (1977) Role of apolipoprotein A-I in the structure of human serum high density lipoproteins. Reconstitution studies, *J. Biol. Chem. 252*, 1208−1216.
21. Pittman, R. C., Glass, C. A., Atkinson, D. A., and Small, D. M. (1987) Synthetic high density lipoprotein particles. Application to studies of the apoprotein specificity for selective uptake of cholesterol esters, *J. Biol. Chem. 262*, 2435−2442.
22. Fang, Y., Gursky, O., and Atkinson, D. (2003) Structural studies of N- and C-terminally truncated human apolipoprotein A-I, *Biochemistry 42*, 13260−13268.
23. Gorshkova, I. N., Liu, T., Zannis, V. I., and Atkinson, D. (2002) Lipid-free structure and stability of apolipoprotein A-I: probing the central region by mutation, *Biochemistry 41*, 10529−10539.
24. Saito, H. S., Dhanasekaran, P., Nguyen, D., Holvoet, P., Lund-Katz, S., and Phillips, M. C. (2003) Domain structure and lipid interaction in human apolipoproteins A-I and E, a general model, *J. Biol. Chem. 278*, 23227−23232.
25. Palgunachari, M. N., Mishra, V. K., Lund-Katz, S., Phillip, M. C., Adeyeye, S. O., Alluri, S., Anantharamaiah, G. M., and Segrest, J. P. (1996) Only the two end helixes of eight tandem amphipathic helical domains of human apoA-I have significant lipid affinity. Implications for HDL assembly, *Arterioscler., Thromb., Vasc. Biol. 16*, 328−338.
26. Zhu, H., AND Atkinson, D. (2004) Conformation and lipid binding of the N-terminal [1−44] domain of human apolipoprotein A-I, *Biochemistry 43*, 13156−13164.
27. Zhu, H., and Atkinson, D. (2007) Conformation and lipid binding of a C-terminal [198−243] peptide of human apolipoprotein A-I, *Biochemistry 46*, 1624−1634.
28. Chao, Y. (2002) Conformational Studies of a Consensus Sequence Peptide (CSP) and a Real Sequence Peptide (RSP) of Apolipoproteins by Circular Dichroism and X-ray Crystallography, Ph.D. Thesis, Department of Physiology and Biophysics, Boston University School of Medicine, Boston, MA.
29. Narayanaswami, V., and Ryan, R. O. (2000) Molecular basis of exchangeable apolipoprotein function, *Biochim. Biophys. Acta 1483*, 15−36.
30. Saito, H., Lund-Katz, S., and Phillips, M. C. (2004) Contributions of domain structure and lipid interaction to the functionality of exchangeable human apolipoproteins, *Prog. Lipid Res. 43*, 350−380.
31. Davidson, W. S., Hazlett, T., Mantulin, W. W., and Jonas, A. (1996) The role of apolipoprotein AI domains in lipid binding, *Proc. Natl. Acad. Sci. U.S.A. 93*, 13605−13610.
32. Saito, H., Dhanasekaran, P., Nguyen, D., Deridder, E., Holvoet, P., Lund-Katz, S., and Phillips, M. C. (2004) α-Helix formation is required for high affinity binding of human apolipoprotein A-I to lipids, *J. Biol. Chem. 279*, 20974−20981.
33. Rogers, D. P., et. al. (1998) Structure analysis of apolipoprotein A-I: Effects of amino- and carboxy-terminal deletions on the lipid-free structure, *Biochemistry 37* (3), 945−955.
34. Mishra, V. K., Palgunachari, M. N., Datta, G., Phillips, M. C., Lund-Katz, S., Adeyeye, S. O., Segrest, J. P., and Anantharamaiah, G. M. (1998) Studies of synthetic peptides of human apolipoprotein A-I containing tandem amphipathic α-helixes, *Biochemistry 37*, 10313−10324.
35. Phillips, M. C., and Krebs, K. E. (1986) Studies of apolipoproteins at the air-water interface, *Methods Enzymol. 128*, 387−403.
36. Krebs, K. E., Phillips, M. C., and Sparkes, C. E. (1983) A comparison of the surface activities of rat plasma apolipoproteins C-II, C-III-0, C-III-3, *Biochim. Biophys. Acta 751*, 470−473.
37. Shen, B. W., and Scanu, A. M. (1980) Properties of human apolipoprotein A-I at the air-water interface, *Biochemistry 19*, 3643−3650
38. Krebs, K. E., Ibdah, J. A., and Phillips, M. C. (1988) A comparison of the surface activities of human apolipoproteins A-I and A-II at the air/water interface, *Biochim. Biophys. Acta 959*, 229−237.
39. Ibdah, J. A., and Phillips, M. C. (1988) Effects of lipid composition and packing on the adsorption of apolipoprotein A-I to lipid monolayers, *Biochemistry 27*, 7155−7162.
40. Ibdah, J. A., Lund-Katz, S., and Phillips, M. D. (1989) Molecular packing of high-density and low-density lipoprotein surface lipids and apolipoprotein A-I binding, *Biochemistry 28*, 1126−1133.
41. Ibdah, J. A., Krebs, K. E., and Phillips, M. C. (1989) The surface properties of apolipoproteins A-I and A-II at the lipid/water interface, *Biochim. Biophys. Acta 1004*, 300−308.
42. Weinberg, R. B., Ibdah, J. A., and Phillips, M. C. (1992) Adsorption of apolipoprotein A-IV to phospholipid monolayers spread at the air/water interface. A model for its labile binding to high density lipoproteins, *J. Biol. Chem. 267*, 8977−8983.
43. Weinberg, R. B., Cook, V. R., DeLozier, J. A., and Shelness, G. S. (2000) Dynamic interfacial properties of human apolipoproteins A-IV and B-17 at the air/water and oil/water interface, *J. Lipid Res. 41*, 1419−1427.
44. Datta, G., Chaddha, M., Hama, S., Navab, M., Fogelman, A. M., Garber, D. W., Mishra, V. K., Epand, R. M., Epand, R. F., Lund-Katz, S., Phillips, M. C., Segrest, J. P., and Anantharamaiah, G. M. (2001) Effects of increasing hydrophobicity on the physical-chemical and biological properties of a class A amphipathic helical peptide, *J. Lipid Res. 42*, 1096−1104.
45. Wang, L., Atkinson, D., and Small, D. M. (2003) Interfacial Properties of an Amphipathic α-Helix Consensus Peptide of Exchangeable Apolipoproteins at Air/Water and Oil/Water Interfaces, *J. Biol. Chem. 278*, 37480−37491.
46. Wang, L., and Small, D. M. (2004) Interfacial properties of amphipathic β strand consensus peptides of apolipoprotein B at oil/water interfaces, *J. Lipid Res. 45*, 1704−1715.
47. Wang, L., Atkinson, D., and Small, D. M. (2005) The Interfacial Properties of ApoA-I and an Amphipathic α-Helix Consensus Peptide of Exchangeable Apolipoproteins at the Triolein/Water Interface, *J. Biol. Chem. 280*, 4154−4165.
48. Wang, L., Walsh, M. T., and Small, D. M. (2006) Apolipoprotein B is conformationally flexible but anchored at a triolein/water interface: A possible model for lipoprotein surfaces, *Proc. Natl. Acad. Sci. U.S.A. 103*, 6871−6876.
49. Labourdenne, S., Gaudry-Rolland, N., Letellier, S., Lin, M., Cagna, A., Esposito, G., Verger, R., and Rivière, C. (1994) The oil-drop tensiometer: potential applications for studying the kinetics of (phospho)lipase action, *Chem. Phys. Lipids 71*, 163−173.
50. Adam, N. K. (1941) *The Physics and Chemistry of Surfaces*, 3rd ed., pp 107−115, Oxford University Press, London.
51. Benjamins, J., and Lucassen-Reynders, E. H. (1998) Surface dilational rheology of proteins adsorbed at air/water and oil/water interfaces, in *Proteins at Liquid Interfaces* (Möbius, D., and Miller, R., Eds.) pp 341−384, Elsevier, Amsterdam.
52. Benjamins, J., Cagna, A., and Lucassen-Reynders, E. H. (1996) Viscoelastic properties of triacylglycerol/water interfaces covered by proteins, *Colloids Surf. 114*, 245−254.

53. Brouillette, C. G., Jones, J. L., Ng, T. C., Kercret, H., Chung, B. H., and Segrest, J. P. (1984) Structural studies of apolipoproteinA-I/phosphatidylcholine recombinants by high-field proton NMR, nondenaturing gradient gel electrophoresis, and electron microscopy, *Biochemistry 23*, 359−367.
54. Saito, H., Dhanasekaran, P., Baldwin, F., Weisgraber, K. H., Lund-Katz, S., and Phillips, M. C. (2001) Lipid binding-induced conformational change in human apolipoprotein E. Evidence for two lipid-bound states on spherical particles, *J. Biol. Chem. 276*, 40949−40954.
55. Small, D. M., and Phillips, M. C. (1992) A technique to estimate the apparent surface pressure of emulsion particles usingapolipoproteins as probes, *Adv. Colloid Interface Sci. 41*, 1−8.
56. Engleman, D. M., Steitz, T. A., and Goldman. A. (1986) Identifying nonpolar transbilayer helices in amino acid sequences of membrane proteins, *Annu. Rev. Biophys. Biophys. Chem. 15*, 321−353.

BI7010114